Published in final edited form as:
Clin Cancer Res. 2005 December 15; 11(24 Pt 1): 8856–8865. doi:10.1158/1078-0432.CCR-05-1365.

Effect of Repetitive Administration of Doxorubicin-Containing Liposomes on Plasma Pharmacokinetics and Drug Biodistribution in a Rat Brain Tumor Model

Robert D. Arnold, **Donald E. Mager**, **Jeanine E. Slack**, and **Robert M. Straubinger**
Department of Pharmaceutical Sciences, University at Buffalo, State University of New York, Amherst, New York

Abstract

Purpose—The incorporation of doxorubicin in long-circulating sterically stabilized liposomes (SSL-DXR) alters the pharmacokinetics and biodistribution of doxorubicin and therefore has the potential to alter the pharmacologic properties of doxorubicin. Previously, we showed that repetitive administration of SSL-DXR alters tumor vascular permeability.

Experimental Design—Here, we investigated the effect of weekly i.v. injections of SSL-DXR on plasma pharmacokinetics and drug biodistribution in the orthotopic 9L rat brain tumor model.

Results and Conclusions—The pharmacokinetics of free doxorubicin (5.67 mg/kg) did not change with repeat dosing. In contrast, drug concentrations in plasma and brain tumor increased and deposition in liver and spleen decreased after administration of the second of two weekly doses of SSL-DXR. Noncompartmental analysis and descriptive pharmacokinetic models were created to test hypotheses relating to the mechanisms responsible for alterations in SSL-DXR deposition. The analysis suggested that weekly administration of SSL-DXR significantly ($P < 0.05$) decreased the plasma elimination rate of SSL-DXR (34%) and decreased drug deposition in liver (2-fold) and spleen (3.5-fold). The pharmacokinetic model that best captured the observed 2.5-fold increase in tumor uptake of SSL-DXR mediated by repeat dosing was one that hypothesized that the rates of drug influx/efflux into tumor were increased by the first dose of SSL-DXR. Models that accounted only for residual drug deposited in the tissue or blood by the first weekly injection provided inferior fits to the data. Thus, the effects of repetitive dosing on SSL-DXR deposition in tumor are consistent with a treatment-mediated alteration of tumor vascular permeability.

The chemotherapy of solid tumors represents a difficult clinical challenge, and pathophysiologic, pharmacologic, and pharmaceutical problems can contribute to therapeutic failure. Poor perfusion, a tortuous and poorly permeable vasculature, high tumor interstitial pressure, and development of drug resistance are tumor properties that hinder drug extravasation, penetration, and retention (1,2). Limited circulating half-life, rapid metabolism, and poor intrinsic tissue permeability are drug properties that limit effectiveness. Nanoparticulate drug carriers, such as liposomes, can alter the pharmacology of encapsulated agents and offer a means to overcome some hindrances to effective therapy. One promising drug carrier formulation consists of doxorubicin loaded into sterically stabilized liposomes, and this formulation is approved as a clinical product in the United States and elsewhere (Doxil/Caelix). It is approved for HIV-related Kaposi's sarcoma, refractory metastatic carcinoma of the ovary, and metastatic breast cancer.

Requests for reprints: Robert M. Straubinger, Department of Pharmaceutical Sciences, University at Buffalo, State University of New York, 539 Cooke Hall, Amherst, NY 14260-1200. Phone: 716-645-2844, ext. 243; Fax: 716-645-3693; rms@buffalo.edu..

Marked differences in the pharmacokinetics of doxorubicin are observed for sterically stabilized liposomal doxorubicin (SSL-DXR) compared with free drug (3). Alterations in doxorubicin circulation half-life and biodistribution along with overall tumor exposure to drug are believed to be responsible for the increased antitumor efficacy and reduced toxicity of SSL-DXR in animal models (3–6). Recently, we observed that repetitive administration of SSL-DXR increased vascular permeability of i.c. rat 9L brain tumors to albumin and increased tumor drug deposition (7). The SSL-DXR dose and schedule of administration that exerted these effects also mediated a 30% extension in life span, whereas free doxorubicin, which did not alter tumor vascular permeability, was no more efficacious than saline (5). Hypotheses to explain the phenomenon of enhanced tumor drug deposition on repetitive administration of SSL-DXR include (*a*) alterations in drug plasma pharmacokinetics as a result of repetitive administration, (*b*) simple additive accumulation of residual drug from repetitive treatments, or (*c*) alterations in the vascular barrier properties of the tumor leading to increased influx or decreased efflux of carrier-encapsulated drug.

The effect of lipid dose and frequency of administration on liposome pharmacokinetics and biodistribution are poorly understood. Repetitive dosing can alter liposome circulation time and clearance in complex ways (8–10). Low doses of “empty” sterically stabilized liposomes (<5 Amol lipid/kg) increased the elimination of subsequent low doses of liposomes but had no effect on the clearance of larger lipid doses (e.g., 50 μmol lipid/kg; refs. 8,11,12). The accelerated clearance of low-dose sterically stabilized liposomes from plasma was correlated with an increase in liposome uptake by the liver and spleen (8), consistent with the induction of low-capacity, saturable clearance mechanisms.

The encapsulated drug itself also has effect on the pharmacokinetics of liposomes (11); treatment of animals with drug-free sterically stabilized liposomes resulted in accelerated elimination of SSL-DXR given 1 week later, but this effect on clearance was not observed if the order of administration was reversed. These data suggest that the encapsulated doxorubicin may also affect liposome clearance mechanisms.

The effect of repetitive administration of higher, more therapeutically relevant doses of SSL-DXR on pharmacokinetics, toxicity, and antitumor efficacy also has been examined (10). Weekly and biweekly administration increased the circulation half-life of doxorubicin, and the rate of doxorubicin elimination from plasma was reduced. However, the effect on plasma elimination rate was more variable when animals were dosed at 4-week intervals, suggesting that an extended interval between doses allowed recovery or decay of the accelerated clearance mechanisms. The 4-week interval dosing regimen also resulted in a reduction in the toxicity of SSL-DXR as indicated by a lower incidence of palmar-plantar erythrodysesthesia lesions. Antitumor efficacy studies supported the concept that larger doses given less frequently (18 mg/kg q2w ×2) were therapeutically superior to smaller doses given more frequently (4.5 mg/kg q3d ×4; ref. 10). Thus, the interplay of dose, pharmacokinetics, and pharmacodynamics are both variable and poorly understood for this novel carrier formulation.

Here, we investigated the effect of repeated weekly doses of SSL-DXR on plasma kinetics and drug biodistribution in a disease model. Rats bearing orthotopic (i.c.) 9L gliosarcoma brain tumors received either one or two weekly doses of free or SSL-DXR. A highly sensitive and selective liquid chromatography-tandem mass spectroscopy assay (13) was used to detect doxorubicin in small-volume samples and to discriminate doxorubicin from inactive and active metabolites that are not resolve by most alternative methods of assay. Pharmacokinetic models were developed and applied to the doxorubicin biodistributional data to test mechanistic hypotheses underlying the observed increase of tumor doxorubicin deposition following weekly redosing with SSL-DXR.

Materials and Methods

Materials and reagents

Doxorubicin (>99% purity) was a gift from Vinchem (Chatham, NJ) and Pharmacia Italia S.p.A. (Milan, Italy). Distearoylphosphatidylcholine and distearoylphosphatidylethanolamine conjugated to 2-kDa methoxy[polyethyleneglycol] were from Avanti Polar Lipids (Alabaster, AL). Cholesterol was purchased from Sigma (St. Louis, MO) and recrystallized thrice from methanol before use. All chemicals and solvents were of analytic or high-performance liquid chromatography grade unless otherwise stated. Heparin sodium for injection USP (5,000 units/mL) was from Elkin-Sinn, Inc. (Cherry Hill, NJ). The rat 9L gliosarcoma cell line, designated as 9L-72, was obtained from Dr. D. Deen (Brain Tumor Research Center, University of California at San Francisco, San Francisco, CA) and maintained in DMEM (Invitrogen, Faraday, CA) supplemented with 10% fetal bovine serum.

Preparation of doxorubicin liposomes

SSL-DXR were prepared from distearoylphosphatidylcholine/cholesterol/methoxy [polyethyleneglycol]-distearoylphosphatidylethanolamine in a 9:5:1 mole ratio using a remote loading procedure (6,14,15); this procedure involves the accumulation of drug into preformed liposomes using combined pH and electrochemical gradients and was modified from the literature as described previously (5). Briefly, liposomes containing 250 mmol/L ammonium sulfate (pH 5.0) were extruded six to eight times through stacked 0.08-Am polycarbonate filters at 60°C using a water-jacketed high-pressure extruder (Northern Lipids, Vancouver, British Columbia, Canada). Unencapsulated ammonium sulfate was removed by dialysis against hypertonic sucrose (500 mOsmol) at 4°C. A 10 mg/mL doxorubicin solution in 10% (w/v) sucrose was prepared, warmed to 65°C, and incubated with the preformed vesicles for 60 minutes at 65°C with intermittent vortex mixing. The phospholipid concentration was determined using an assay for inorganic phosphate following acid hydrolysis (16). Free (unencapsulated) drug was removed by dialysis and the formulation was sterilized by filtration through 0.2-μm filters. Doxorubicin concentrations were determined from absorbance at 490 nm using a spectrophotometer (Cary 300, Varian, Inc., Palo Alto, CA) assuming ε_a = 12,500 M^{-1} cm^{-1} (3). The final concentration of doxorubicin was typically 2 mg/mL, with a drug/lipid ratio 0.22:1.0 (mol:mol). Encapsulation efficiencies were >95%. Liposomes had a mean particle diameter of 80 to 110 nm as determined using a Nicomp model 380 dynamic light scattering particle size analyzer (Santa Barbara, CA). SSL-DXR preparations were purged with nitrogen and stored in the dark at 4°C until use.

Plasma pharmacokinetics and tissue biodistribution

9L brain tumor implantation—Rat 9L gliosarcoma rat brain tumor cells were implanted stereotaxically in the caudate putamen brain region of Fisher 344 male rats as described previously (5). Briefly, rats were anesthetized with an i.m. injection of 50 mg/kg ketamine and 5 mg/kg xylazine and placed in a small animal stereotaxic frame (Kopf model 902, Tujunga, CA). A suspension containing 4×10^4 9L cells in 3 to 5 μL DMEM buffered with 20 mmol/L HEPES was injected using a sharp 26-gauge Hamilton syringe inserted through a burr hole in the skull to a depth of 4.5 mm from the exposed dura, 1.5 mm anterior and 2.4 mm lateral to bregma. The burr hole was filled with Gelfoam (Upjohn, Kalamazoo, MI) and the scalp was closed with surgical staples.

Doxorubicin biodistribution—Free or SSL-DXR was given at 5.67 mg/kg by tail vein injection. For rats treated with SSL-DXR, the total lipid given was <16 μmol/dose. Free drug was given at an equivalent concentration. Two groups of animals received a single treatment, on either day 7 or 14 after tumor implantation, when the tumor weights were 20 or 60 mg, respectively. A third group was treated on both days 7 and 14.

The temporal profile of tumor drug concentrations was determined after single and weekly repeated treatments. Because of pharmacokinetic differences between the two formulations, animals treated with free doxorubicin were sacrificed at 0.5 to 4 hours after administration, and those treated with SSL-DXR were sacrificed at 1 to 168 hours after administration. At time of sacrifice, a midline incision was made in the abdomen. Blood was flushed from the circulatory system by severing the inferior vena cava and infusing 100 mL heparinized (5 units/mL) saline through the left ventricle. The tumor, contralateral brain hemisphere, liver, spleen, heart, and lung were excised rapidly, weighed, frozen in liquid nitrogen, and stored at –80°C until analysis.

Plasma pharmacokinetics—Rats were anesthetized with 90 mg/kg ketamine and 9 mg/kg xylazine i.m. A PE-50 polyethylene cannula was inserted into the jugular vein and exteriorized through a 3- to 5-mm slit between the scapulae. Three days after surgery, rats were treated with 5.67 mg/kg free or SSL-DXR by i.v. injection via the tail vein. Blood samples of 100 to 200 μL were collected into heparinized syringes at various times and iced immediately. Plasma was collected by centrifugation at 1,200 × *g* for 10 minutes at 4°C, frozen in liquid nitrogen, and stored at –80°C until analysis. Hematocrit concentrations were determined routinely to ensure animals were within 15% of pretreatment values (data not shown).

Animal handling, surgery, and postsurgical care were completed following a protocol approved in advance by the Institutional Animal Care and Use Committee of the University at Buffalo in accordance with the USPHS Policy on Humane Care and Use of Laboratory Animals, updated 1996. Animals were provided a standard rat chow diet (Harlan Teklad Rodent Diet 2016, Indianapolis, IN) and water *ad libitum*.

Doxorubicin analysis

Doxorubicin was extracted from plasma and tissue samples and quantified by liquid chromatography-tandem mass spectroscopy as described previously (13). An electrospray ionization source was used on an ABI/Sciex API3000 triple-quadrapole mass spectrometer (ABI, Inc., Foster City, CA) following chromatographic separation using an Agilent model 1100 high-performance liquid chromatography system (Palo Alto, CA). The assay was linear over the concentration range of 0.125 to 10,000 nmol/L and permitted identification of doxorubicin and its metabolites (e.g., doxorubicinol and doxorubicinone). Differences in tissue or tumor drug deposition were tested using a stepwise, two-way ANOVA followed by a *post hoc* Bonferroni *t* test in SAS version 8.02 for Windows (Cary, NC). Differences were considered significant at $P < 0.05$.

Pharmacokinetic analysis

Noncompartmental analysis—Noncompartmental analysis of data for animals treated with one or two weekly doses was done using WinNonlin version 2.1 (Pharsight, Mountain View, CA). Variables included maximum plasma concentration (C_{max}), terminal elimination rate (k), half-life ($t_{1/2}$), area under the plasma concentration-time curve (AUC), apparent volume of distribution (V), and total systemic clearance (CL). The AUC after single or repetitive administration of SSL-DXR was estimated using the log-trapezoidal function (17). In repetitive administration, detectable SSL-DXR remained in the blood and tumor after 7 days (168 hours). The contribution of this residual drug to the AUC calculated for the second dose (in repetitively treated animals) was investigated by subtracting from the AUC for the second dose, the $AUC_{168\text{-}240\ hours}$ observed for the single dose. Estimated variables were compared using ANOVA followed by a *post hoc* Bonferroni *t* test in SAS. Differences were statistically significant at Ps < 0.05.

Pharmacokinetic modeling—An empirical pharmacokinetic model was developed to describe the plasma concentration-time profile after repetitive administration of SSL-DXR. The amount of drug in plasma (A_p) was modeled using a one-compartment model:

$$\frac{dA_p}{dt} = -(k_i - \alpha \cdot t) \cdot A_p \quad \text{(A)}$$

where k_i is the initial first-order rate of elimination and α is an incremental change in k_i with time (t). The concentration of doxorubicin in plasma was calculated as $C_p = A_p/V$, where V is the apparent volume of distribution. The pharmacokinetic variables were estimated from (*a*) naive pooled data, (*b*) naive averaged data, and (*c*) standard two-stage data analysis using the nonlinear regression analysis package ADAPT II (18) and employing the maximum likelihood estimator. The variance model was specified as $\sigma_c^2=(\sigma_1+\sigma_2 Y)^2$, where $\sigma_1 = 0$, σ_2 is an estimated variable, and Y is a model-predicted value. Visual inspection and objective criteria (Akaike information criteria, Schwarz criteria, sum of squares, and estimator criterion value) were used to evaluate goodness-of-fit and model selection (19).

Brain tumor concentrations of doxorubicin were fitted using a one-compartment model:

$$\frac{dC_{tumor}}{dt} = X_{ct} \cdot k_{ct} \cdot C_{plasma} - X_{tc} \cdot k_{tc} \cdot C_{tumor} \quad \text{(B)}$$

where C_{tumor} is the concentration of doxorubicin in tumor, k_{ct} and k_{tc} are first-order rate constants for bidirectional drug transfer between central (plasma) and tumor compartments, and C_{plasma} is the doxorubicin concentration in plasma. The final estimated variables obtained from the pharmacokinetic model (Eq. A) were fixed and Eq. A was used as a driving function for the brain tumor deposition model (Eq. B). Multiplicative coefficients (scaling factors) that accommodate a single stepwise change in variable values from different cohorts were used to estimate the magnitude of change in the tumor doxorubicin influx (X_{ct}) or efflux (X_{tc}) rate mediated by repetitive administration of SSL-DXR. Data from each treatment group were fitted simultaneously with ADAPT II (18) using the maximum likelihood estimator and the identical variance model as was used for the pharmacokinetic analysis.

Results

Biodistribution of doxorubicin

Brain tumor deposition—The effect of weekly dosing of free or SSL-DXR on deposition in tumor and tissues was examined in rats bearing i.c. 9L brain tumors. Animals were treated as described in Materials and Methods; single-treatment cohorts received doxorubicin on day 14 after tumor implantation, whereas other cohorts were dosed both 7 and 14 days after implantation.

Figure 1 shows tumor and tissue accumulation of free and SSL-DXR. Following i.v. administration of free doxorubicin on day 14, peak tumor concentrations of 80 to 240 ng/g tumor were observed 1 to 4 hours after injection (Fig. 1). In animals treated on both days 7 and 14, doxorubicin tumor deposition following the day 14 dose was 1.58-fold higher than naive animals receiving their first dose on that day based on naive averaged data (n = 27 animals) analysis (data not shown). However, this change was not significant ($P > 0.05$).

For animals treated with a single dose of SSL-DXR (on day 14), the maximum tumor drug deposition was observed 24 hours after administration and averaged 835 ng/g tumor (Fig. 1).

For animals treated with SSL-DXR at weekly intervals (days 7 and 14), the maximum drug concentration was observed within 8 hours of the second (day 14) dose and averaged 1,830 ng/g tumor. Table 1 shows the effect of repeated weakly treatments with SSL-DXR on tumor deposition. The analysis was done using naive averaged data (n = 27 animals). Over 72 hours after administration, the day 14 dose of SSL-DXR in animals dosed weekly (days 7 and 14) resulted in tumor drug concentrations 2-to 3-fold greater than observed in naive animals receiving their first dose of SSL-DXR on day 14. The second weekly treatment of redosed animals resulted in a mean doxorubicin brain tumor concentration of 1,760 ng/mL compared with 769 ng/mL in naive animals (Table 1). This 2.3-fold increase in doxorubicin deposition with redosing dosing was significant at $P < 0.001$.

Selectivity of sterically stabilized liposomal doxorubicin effect on drug deposition—Selective enhancement of drug deposition in the target tissue is an important consideration given the toxicity of anticancer agents to sensitive nontarget tissues. Weekly dosing with free or SSL-DXR (on days 7 and 14) did not change the deposition of either in the normal brain compared with a single dose (on day 14). However, tumor/brain ratios of drug did change depending on formulation and schedule of administration. After a single dose of SSL-DXR (day 14), drug deposition was 15-fold greater in tumor than in normal brain (Fig. 1); this differential increased to 46-fold in animals receiving two weekly doses (days 7 and 14). After a single (day 14) dose of free doxorubicin, drug deposition was 3.7-fold greater in tumor than in brain, and the tumor/brain deposition ratio was 3.9-fold in animals receiving two (days 7 and 14) doses of free doxorubicin; this difference was not significant.

The effect of formulation and treatment schedule on doxorubicin deposition in other tissues was also investigated. The liver represents the principal organ for the elimination of both free and liposome-encapsulated doxorubicin. Following free doxorubicin administration, liver concentrations rapidly reached a peak of 30 μg/g and then fell over 4 hours to 10 μg/g (Fig. 1). Animals that received two weekly doses (days 7 and 14) showed no significant difference in liver deposition after the day 14 dose. In contrast, liver concentrations were 15 μg/g in animals receiving a single (day 14) administration of SSL-DXR but were reduced 52% in animals dosed twice (days 7 and 14), and this change was significant at $P < 0.05$.

Formulation- and treatment-mediated differences in drug deposition were also observed in the spleen, a major organ of liposome clearance. Per gram of tissue, the spleen had 10-fold greater uptake of SSL-DXR than did the liver (Fig. 1). Compared with naive animals receiving their first dose of SSL-DXR on day 14, those receiving a second weekly dose of SSL-DXR (days 7 and 14) showed a 72% decrease in spleen deposition, which was significant at $P < 0.05$. Deposition of free doxorubicin in spleen was not altered by weekly redosing.

Doxorubicin deposition in lung was higher in animals treated with free doxorubicin (18.2 μg/g lung) than with SSL-DXR (10.9 μg/g lung). Weekly redosing dosing did not have a significant effect on the lung deposition of either formulation.

The peak deposition of doxorubicin in heart, an organ of cumulative doxorubicin toxicity, was 3-fold higher following a single (day 14) treatment with free doxorubicin (15.3 μg/g heart at 0.5 hour) than after SSL-DXR (5.3 μg/g heart at 48 hours; this difference was significant at $P < 0.001$) (Fig. 1). Heart deposition was not increased in animals that were redosed (days 7 and 14) with either formulation.

Plasma pharmacokinetics

Following a single injection, free doxorubicin was eliminated rapidly from the plasma and exhibited polyexponential kinetics (Fig. 2A). In animals dosed on days 7 and 14 with free doxorubicin, no difference in the circulation time profile or rate of elimination was observed

after the second treatment (Fig. 2A). A long (48-58 hours) terminal half-life was observed, but it accounted for <20% of the total $AUC_{(0-\infty)}$. This observation is characteristic of drugs that are bound extensively to proteins and/or released from tissue over a prolonged time (20,21).

Encapsulation of doxorubicin in sterically stabilized liposomes radically altered the pharmacokinetics compared with free drug (Fig. 2A). Therefore, both noncompartmental and compartmental analyses were done to analyze plasma temporal profiles of SSL-DXR and to investigate mechanisms by which repetitive dosing might preferentially alter tissue accumulation of drug.

The temporal profile of SSL-DXR given on day 14 appeared similar in naive animals receiving their first treatment and in animals that were dosed on both days 7 and 14; in both cases, SSL-DXR was eliminated from the plasma in a monoexponential fashion (Fig. 2). However, noncompartmental analysis (Table 2) revealed that the plasma elimination rate was 0.020/h in naive animals receiving their first dose of SSL-DXR (day 14) and 0.013/h in animals receiving their second weekly dose on day 14. This 34% decrease in the plasma elimination rate was significant ($P < 0.05$). The terminal half-life of doxorubicin was 55 hours in twice-dosed (days 7 and 14) animals and 36 hours for naive animals receiving their first SSL-DXR dose on day 14 (Table 2; Fig. 2A). This difference also was significant ($P < 0.05$).

Total systemic clearance was 24% lower after day 14 dosing in animals receiving two weekly doses of SSL-DXR (0.733 versus 0.560 mL/h/kg), and the AUC was increased 29% (7.54-9.74 mg h/mL) in redosed animals. However, neither changes in AUC nor clearance were significant ($P > 0.05$). The apparent volume of distribution in animals dosed both singly (day 14) and repetitively (days 7 and 14) with SSL-DXR was 40.0 mL/kg, within the range reported for the total plasma volume of normal rats (30-50 mL/kg body weight; ref. 22).

Descriptive pharmacokinetic models were developed to test whether it was necessary to hypothesize alterations in fundamental biodistributional or elimination processes in order for the models to characterize the plasma concentration-time profiles of animals treated singly (day 14) versus twice (days 7 and 14) with SSL-DXR. A standard one-compartment pharmacokinetic model with linear first-order elimination was evaluated first. The use of a constant elimination rate term (k) was found to overestimate the observed plasma concentrations in the terminal phase of naive animals receiving a single SSL-DXR treatment and to underestimate plasma concentrations in animals receiving the second of two weekly doses (Fig. 2B, *dashed line*).

The one-compartment model was modified such that the initial first-order rate term (k) decreased in response to the first (day 7) SSL-DXR treatment according to the proportionality constant α. When fit simultaneously to all data (for both singly and twice-treated animals), this model predicted that the initial rate (k) for animals on day 7 was 0.02/h and decreased to a value of 0.013/h by day 14, 1 week after the first SSL-DXR administration (Table 2). The predicted values for these variables were in agreement with the values obtained by noncompartmental analysis (Table 2). The α term, representing the incremental change in the elimination rate as a function of time, was found to be small ($2.8 \times 10^{-5}/h^2$), but it improved overall model fitting criteria. The estimated volume of SSL-DXR distribution was 40.7 to 43.0 mL/kg, within the range published for the average plasma volume of the rat (22) and in excellent agreement with the values obtained by noncompartmental analysis. Thus, incorporation into the pharmacokinetic model of a treatment-dependent change in the plasma elimination rate, triggered by the initial (day 7) SSL-DXR dose, enabled the construction of a model that accurately captured the day 14 plasma data for singly and twice-treated animals.

Plasma concentrations drive tumor and organ accumulation of SSL-DXR following i.v. administration. Therefore, having developed an accurate model that simultaneously captured

plasma concentrations for animals treated once (day 7 or day 14) versus twice (days 7 and 14) with SSL-DXR, it was possible to explore several pharmacokinetic models designed to investigate factors underlying the observed increase in tumor deposition of SSL-DXR following repetitive treatment. The models tested several specific hypotheses: (*a*) that the increased tumor deposition was the result of the treatment-mediated increase in the circulating half-life of SSL-DXR, which allowed a greater proportion of liposomes to extravasate; (*b*) that deposition was not enhanced by weekly redosing, and residual drug from the initial (day 7) treatment could account for the observed tumor concentrations of SSL-DXR; or (*c*) that the tumor vascular barrier properties were altered by the initial (day 7) treatment.

A one-compartment pharmacokinetic model was developed to describe drug transfer from the plasma to the brain tumor (Fig. 3A). The model incorporated rate constants for tumor influx and efflux of doxorubicin, and this feature permitted a more detailed examination of possible changes in vascular permeability mediated by repeated weekly doses of SSL-DXR. The plasma pharmacokinetic model described above was used as a driving function to supply drug concentrations in the tumor vasculature.

Pharmacokinetic models that assumed fixed rates of tumor influx and efflux did well for animals treated singly (day 7 or 14) but did poorly when fitting all data simultaneously (i.e., animals dosed on day 7, day 14, and days 7 and 14). Residual drug was detected on day 14 in both tumor and plasma of animals treated on day 7. Models were developed to account for this residual drug in plasma (first hypothesis) or in tumor (second hypothesis) but failed to capture the observed tumor concentration-time profiles for redosed (days 7 and 14) animals (data not shown).

An alternative pharmacokinetic model was created in which repetitive administration was assumed to alter drug influx and efflux rates for tumor (Eq. B; Fig. 3A). Data for three SSL-DXR treatment regimens were fitted simultaneously: animals treated once (*a*) on day 7 or (*b*) on day 14 and (*c*) animals treated twice at weekly intervals (days 7 and 14; Fig. 3B). Models in which either influx or efflux rates did not respond to SSL-DXR treatment resulted in poor fits of these three data sets. The model that best fit data for both singly and twice-treated animals incorporated terms describing treatment-dependent alterations in the tumor drug influx and efflux rates (Fig. 3A).

The optimal pharmacokinetic model suggested that the initial (day 7) SSL-DXR treatment increased the subsequent rate of drug influx into the brain tumor by 4.1-fold and the rate of efflux by 2.2-fold (Table 3). The disproportion between these rate constants suggests a mechanism by which tumor deposition of SSL-DXR would increase on repeated administration.

This more optimal model captured the observed data well, and the AUC for doxorubicin in the tumor (AUC_{tumor}) predicted by the model was in close agreement with the AUC_{tumor} calculated from the means of the data points (Table 1). The AUC_{tumor} calculated from the data was 2.3-fold greater in animals receiving the second of two weekly doses of SSL-DXR than in naive animals receiving their first dose (129 versus 57.5 μg h/g, respectively; Table 1; Fig. 3B). For the model prediction, if the prior administration of SSL-DXR was hypothesized to alter tumor influx rates, then the model predicted an AUC_{tumor} 2.5-fold higher for animals receiving the second of two weekly doses of SSL-DXR (159 versus 67.3 μg h/g, respectively; Table 1; Fig. 3B). The optimal model takes into account any residual doxorubicin in tumor or plasma 1 week after the day 7 treatment; under conditions of best fit, residual drug accounted for <4% of the total AUC observed after the second (day 14) administration of SSL-DXR (Fig. 3B). The model also correctly captured the apparent shift in tumor accumulation peak time observed in redosed animals; in naive animals receiving their first dose of SSL-DXR on day 14, peak tumor

concentrations were observed at 24 hours. In contrast, both the data and the optimal model suggested that peak concentrations were reached within 8 hours in animals that had received a dose of SSL-DXR 1 week prior (days 7 and 14).

Discussion

Encapsulation of anthracyclines, such as doxorubicin, in sterically stabilized liposomes significantly increases circulation time, alters tissue and tumor biodistribution, and improves efficacy in animal model systems (3,9,23). Recently, we described the effects of repetitive dosing with SSL-DXR on the survival of i.c. 9L tumors (5) and on the tumor vascular permeability to probes, such as Evans blue, an albumin-binding dye that is commonly employed as a marker for compromise of the blood-brain barrier (7,24). Here, we have investigated the pharmacokinetics of free and SSL-DXR under conditions in which the liposomal formulation mediated both an extension in tumor survival and a selective increase in tumor vascular permeability.

Several significant effects of SSL-DXR were observed in this i.c. tumor model system that were not observed with free doxorubicin. First, the plasma half-life of drug was increased significantly. Second, deposition in the liver and spleen, the major organs for liposome clearance, was decreased. Third, peak concentrations of doxorubicin in heart were 3-fold lower after treatment with SSL-DXR compared with free doxorubicin and the repeated weekly administration did not increase SSL-DXR deposition in the heart. Finally, and perhaps most importantly, repetitive dosing with SSL-DXR increased tumor deposition of doxorubicin significantly, whereas weekly redosing with free doxorubicin did not.

To investigate the multiple, interrelated effects observed with repetitive dosing of SSL-DXR, a series of pharmacokinetic models was developed and tested to estimate the role that each potentially significant factor might play in terms of pharmacokinetics and biodistribution. Quantitative mathematical models represent testable hypotheses that incorporate the possible underlying mechanisms by which these nanoparticu-late carriers alter the pharmacology of the encapsulated therapeutic agent (25–27).

Both noncompartmental analysis and empirical pharmacokinetic models captured well the observed plasma concentration-time profile of doxorubicin; both indicated that repeat dosing with SSL-DXR mediated an increase in the circulation half-life of doxorubicin. A pharmacokinetic model that hypothesized a treatment-mediated decrease in a first-order elimination rate process provided the best simultaneous fit of all data. The model suggested that a significant decrease in the plasma elimination rate resulted from weekly administrations of SSL-DXR.

Several processes may contribute to the observed decrease in plasma elimination rate. Biodistribution data showed that repetitive administration of SSL-DXR decreased deposition in the liver and spleen, the principal organs involved in the clearance of liposomes. Liposomes and other particulate delivery systems undergo removal by the reticuloendothelial system, an innate nonspecific host defense mechanism responsible for the elimination of senescent cells and macromolecules as well as foreign particles, such as pathogens (28–30). Clearance is mediated by the fixed macrophages of the liver, spleen, and lung that constitute the reticuloendothelial system and is assisted by opsonins that facilitate macrophage uptake of foreign particulates (31–33).

The administration of large doses of colloidal particles has been observed to extend liposome circulation times by saturation of the reticuloendothelial system clearance mechanisms (33–36). Here, animals were treated at weekly intervals with 50 μmol lipid/kg, a therapeutically relevant dose that could exert some effect on reticuloendothelial system clearance (10). The

specific role of reticuloendothelial system blockade was not addressed directly in this work but would be consistent with the observed enhancement of SSL-DXR blood levels following repeat dosing.

In animals that received a dose of SSL-DXR a week previously (i.e., on days 7 and 14), the deposition of a subsequent dose of SSL-DXR in 9L i.c. tumors was increased. Several studies suggest that enhanced tumor deposition may be attributed to the increased circulation time of sterically stabilized liposomes in conjunction with a hyperpermeable tumor vasculature (3, 23,37). However, pharmacokinetic analysis of the data from animals treated on days 7 and 14 indicated that a treatment-related decrease in SSL-DXR elimination rates could not explain the observed increase in tumor deposition. Biodistribution data also showed a long-term persistence of drug from SSL-DXR in the tumor. However, pharmacokinetic models that accounted for this accumulation of residual intratumor drug similarly did not provide the best fits for the data obtained from rats treated on days 7 and 14 with SSL-DXR. Finally, modeling supported the conclusion that intratumor concentrations of doxorubicin increased more rapidly in animals that had been treated previously with SSL-DXR and remained elevated for longer than in naive animals.

The hypothesis that best fit the data was one that tested whether weekly dosing increased the tumor vascular permeability. In this pharmacokinetic model, the initial (day 7) SSL-DXR treatment was calculated to increase tumor influx 4-fold and tumor efflux 2-fold. An increase in the tumor influx rate would be consistent with the observed shift in the peak time of tumor accumulation of SSL-DXR in repetitively treated animals, and a disproportionate increase in the tumor influx rate compared with the efflux rate would result in an overall increase in tumor drug deposition.

The mechanisms by which tumor vascular permeability may be altered by repeat weekly dosing with SSL-DXR are not yet clear. Magnetic resonance imaging and functional magnetic resonance imaging suggest that SSL-DXR increases fluid flow within 9L tumors and induces disseminated microhemorrhage (24,38). More recently, we have observed that repetitive administration of SSL-DXR increased tumor vascular permeability to both albumin and liposomes (7). However, permeability to albumin was not increased by SSL-DXR in normal brain, liver, and heart. Moreover, changes in drug deposition or vascular permeability were not found in organs associated with drug-mediated toxicity (e.g., heart) after repetitive treatment with SSL-DXR.

The apparent selectivity of the effect of SSL-DXR on tumor vascular permeability may arise from the intrinsic hyper-permeability of tumors and the enhanced permeability and retention phenomenon (39), in which the pathophysiology of the tumor vasculature presents opportunities for macro-molecular and particulate drug carriers to undergo enhanced deposition in the tumor. We observed previously by fluorescence microscopy that liposomes extravasated sporadically and nonuniformly in i.c. 9L tumors and remained in close proximity to structures that resembled tumor blood vessels (5); others have also shown dense accumulations of sterically stabilized liposomes near tumor vessel walls (40). We hypothesize that this elevated concentration of drug in close proximity to the tumor vasculature exerts an antivascular effect that is progressive, with successive doses increasing the damage to the tumor vasculature. It is not known whether the tumor vascular endothelial cells are affected directly by SSL-DXR deposition or whether local killing of tumor cells surrounding the site of extravasation reduces the chemokine drive that supports the tumor vasculature.

The data presented here confirm that a much smaller fraction of the given dose of SSL-DXR was deposited in the i.c. 9L tumors (0.04-0.20% of injected dose/g tumor) compared with results reported for other tumor models. For example, 5% to 13% of injected dose/g tumor

were achieved in mice bearing s.c. implanted LS174T human colon carcinoma or B16 melanoma tumors (41) and 20% of injected dose/g tumor was achieved in the s.c. Colon-26 murine model (40). Brain tumors expand within a closed cranial compartment and typically develop edema and high interstitial pressures; these anatomic constraints and pathophysiologic characteristics may play a significant role in the much lower SSL-DXR deposition observed here with i.c. 9L tumors. Differences in the tumor microenvironment and in the vascular architecture of orthotopic versus s.c. tumors may also play a contributory role. Nonetheless, in spite of the low fraction of injected SSL-DXR that accumulated in 9L tumors, a significant increase in survival was achieved in animals treated weekly with SSL-DXR, whereas animals treated with free drug or sucrose survived no longer than untreated controls (5). Repetitive dosing with SSL-DXR may progressively increase the tumor vascular permeability in spite of low initial deposition, increasing the penetration of the drug into the tumor.

The pharmacokinetic models developed here did well in capturing the data for two weekly administrations of SSL-DXR. Because of a lack of direct data on tumor influx and efflux rates, we employed an empirically derived model component that is descriptive in nature and consistent with the observed data on liposome clearance *in vivo* (10). However, a potential shortcoming of the model is that it assumes that tumor permeability changes progressively as a function of time and does not account for repair mechanisms that may counteract the effects of treatment on tumor vascular permeability. This shortcoming of the model can be addressed with the acquisition of more extensive data on the time course of tumor vascular barrier compromise and repair.

Importantly, animals treated with SSL-DXR achieved peak brain tumor concentrations 10-fold greater than after administration of free drug, and deposition was increased significantly by repetitive administration of SSL-DXR. At the same time, peak cardiac deposition was 3-fold lower for SSL-DXR than for the free drug and was not increased by repetitive administration. Although the clinical implications of the effects observed here are not yet known, the dose and interval between doses of SSL-DXR may play an important role in toxicities that are observed in the clinic. The observation of positive effects of repetitive dosing on tumor deposition of SSL-DXR suggests a phenomenon that may be optimized for further improvement of therapeutic outcome.

Acknowledgments

We thank our colleague Dr. A. Forrest for assistance with the statistical analysis and D. Soda for assistance with the surgical procedures.

Grant support: National Cancer Institute, NIH grant RO1-CA107570 and Association for the Research of Childhood Cancer (R.M. Straubinger), American Foundation for Pharmaceutical Education predoctoral fellowship (R.D. Arnold), and Pfizer, Inc., and American Foundation for Pharmaceutical Education undergraduate research fellowships (J.E. Slack). The Pharmaceutical Sciences Instrumentation Facility at the University at Buffalo provided access to the fluorescence spectrometer and liquid chromatography-tandem mass spectrometry system, which were obtained with shared equipment grants S10-RR15877 and S10-RR14592, respectively, from the National Center for Research Resources, NIH.

References

1. Jain RK. Vascular and interstitial barriers to delivery of therapeutic agents in tumors. Cancer Metastasis Rev 1990;9:253–66. [PubMed: 2292138]
2. Brown JM, Giaccia AJ. The unique physiology of solid tumors: opportunities (and problems) for cancer therapy. Cancer Res 1998;58:1408–16. [PubMed: 9537241]
3. Gabizon A, Shiota R, Papahadjopoulos D. Pharmacokinetics and tissue distribution of doxorubicin encapsulated in stable liposomes with long circulation times. J Natl Cancer Inst 1989;81:1484–8. [PubMed: 2778836]

4. Siegal T, Horowitz A, Gabizon A. Doxorubicin encapsulated in sterically stabilized liposomes for the treatment of a brain tumor model: biodistribution and therapeutic efficacy. J Neurosurg 1995;83:1029–37. [PubMed: 7490617]
5. Sharma US, Sharma A, Chau RI, Straubinger RM. Liposome-mediated therapy of intracranial brain tumors in a rat model. Pharm Res 1997;14:992–8. [PubMed: 9279878]
6. Gabizon AA. Selective tumor localization and improved therapeutic index of anthracyclines encapsulated in long-circulating liposomes. Cancer Res 1992;52:891–6. [PubMed: 1737351]
7. Arnold RD, Mager DE, Spernyak JA, Mazurchuk RV, Straubinger RM. Tumor antivascular effects of sterically-stabilized doxorubicin-containing liposomes. Proc Am Assoc Cancer Res 2005;46:3800.
8. Dams ET, Laverman P, Oyen WJ, et al. Accelerated blood clearance and altered biodistribution of repeated injections of sterically stabilized liposomes. J Pharmacol Exp Ther 2000;292:1071–9. [PubMed: 10688625]
9. Allen TM, Hansen C. Pharmacokinetics of stealth versus conventional liposomes: effect of dose. Biochim Biophys Acta 1991;1068:133–41. [PubMed: 1911826]
10. Charrois GJ, Allen TM. Multiple injections of pegylated liposomal doxorubicin: pharmacokinetics and therapeutic activity. J Pharmacol ExpTher 2003;306:1058–67.
11. Laverman P, Carstens MG, Boerman OC, et al. Factors affecting the accelerated blood clearance of polyethylene glycol-liposomes upon repeated injection. J Pharmacol ExpTher 2001;298:607–12.
12. Ishida T, Maeda R, Ichihara M, Irimura K, Kiwada H. Accelerated clearance of PEGylated liposomes in rats after repeated injections. J Control Release 2003;88:35–42. [PubMed: 12586501]
13. Arnold RD, Slack JE, Straubinger RM. Quantification of doxorubicin and metabolites in rat plasma and small volume tissue samples by liquid chromatography/electrospray tandem mass spectroscopy. J Chromatogr B AnalytTechnol Biomed Life Sci 2004;808:141–52.
14. Madden TD, Harrigan PR, Tai LC, et al. The accumulation of drugs within large unilamellar vesicles exhibiting a proton gradient: a survey. Chem Phys Lipids 1990;53:37–46. [PubMed: 1972352]
15. Lasic DD, Martin FJ, Gabizon A, Huang SK, Papahadjopoulos D. Sterically stabilized liposomes: a hypothesis on the molecular origin of the extended circulation times. Biochim Biophys Acta 1991;1070:187–92. [PubMed: 1751525]
16. Bartlett GR. Phosphorous assay in column chromatography. J Biol Chem 1959;234:466–8. [PubMed: 13641241]
17. Gibaldi, M.; Perrier, D. Pharmacokinetics. 2nd ed.. Dekker; New York: 1982.
18. D'Argenio, DZ.; Schumitzky, A. ADAPT II user's guide: pharmacokinetic/pharmacodynamic systems analysis software. Biomedical Simulations resource; Los Angeles: 1997.
19. Gabrielsson, JL.; Weiner, DL. Pharmacokinetic and pharmacodynamic data analysis: Concepts and applications. Swedish Pharmaceutical Press; Stockholm, Sweden: 2000.
20. McNamara PJ, Levy G, Gibaldi M. Effect of plasma protein and tissue binding on the time course of drug concentration in plasma. J Pharmacokinet Biopharm 1979;7:195–206. [PubMed: 20218014]
21. MacKichan, JJ. Influenceofproteinbindinganduse of unbound (free) drug concentrations.. In: Evans, WE.; Schentag, JS.; Jusko, WJ., editors. Applied pharmacokinetics, principles of therapeutic drug monitoring. 3rd ed.. AppliedTherapeutics; Vancouver (WA): 1994. p. 5-1-5-48.
22. Waynforth, HB. Experimental and surgical technique in the rat. Academic Press; London: 1980.
23. Papahadjopoulos D, Allen TM, Gabizon A, et al. Sterically stabilized liposomes: improvements in pharmacokinetics and antitumor therapeutic efficacy. Proc Natl Acad Sci U S A 1991;88:11460–4. [PubMed: 1763060]
24. Zhou R, Mazurchuk R, Straubinger RM. Antivasculature effects of doxorubicin-containing liposomes in an intracranial rat brain tumor model. Cancer Res 2002;62:2561–6. [PubMed: 11980650]
25. Derendorf H, Meibohm B. Modeling of pharmacokinetic/pharmacodynamic (PK/PD) relationships: concepts and perspectives. Pharm Res 1999;16:176–85. [PubMed: 10100300]
26. Mager DE, Wyska E, Jusko WJ. Diversity of mechanism-based pharmacodynamic models. Drug Metab Dispos 2003;31:510–8. [PubMed: 12695336]
27. Abdel-Rahman SM, Kauffman RE. The integration of pharmacokinetics and pharmacodynamics: understanding dose-response. Annu Rev Pharmacol Toxicol 2004;44:111–36. [PubMed: 14744241]

28. Ahsan F, Rivas IP, Khan MA, Torres Suarez AI. Targeting to macrophages: role of physicochemical properties of particulate carriers—liposomes and microspheres—on the phagocytosis by macrophages. J Control Release 2002;79:29–40. [PubMed: 11853916]
29. Oh YK, Nix DE, Straubinger RM. Formulation and efficacy of liposome-encapsulated antibiotics for therapy of intracellular *Mycobacterium avium* infection. Antimicrob Agents Chemother 1995;39:2104–11. [PubMed: 8540724]
30. Schiffelers RM, Bakker-Woudenberg IA, Snijders SV, Storm G. Localization of sterically stabilized liposomes in *Klebsiella pneumoniae*-infected rat lung tissue: influence of liposome characteristics. Biochim Biophys Acta 1999;1421:329–39. [PubMed: 10518702]
31. Dijkstra J, van Galen M, Regts D, Scherphof G. Up-take and processing of liposomal phospholipids by Kupffer cells *in vitro*. Eur J Biochem 1985;148:391–7. [PubMed: 3987696]
32. Poste G, Bucana C, Raz A, Bugelski P, Kirsh R, Fidler IJ. Analysis of the fate of systemically administered liposomes and implications for their use in drug delivery. Cancer Res 1982;42:1412–22. [PubMed: 7060015]
33. Oja CD, Semple SC, Chonn A, Cullis PR. Influence of dose on liposome clearance: critical role of blood proteins. Biochim Biophys Acta 1996;1281:31–7. [PubMed: 8652601]
34. Laverman P, Brouwers AH, Dams ET, et al. Preclinical and clinical evidence for disappearance of long-circulating characteristics of polyethylene glycol liposomes at low lipid dose. J Pharmacol Exp Ther 2000;293:996–1001. [PubMed: 10869403]
35. Parr MJ, Bally MB, Cullis PR. The presence of GM1 in liposomes with entrapped doxorubicin does not prevent RES blockade. Biochim Biophys Acta 1993;1168:249–52. [PubMed: 8504161]
36. Souhami RL, Patel HM, Ryman BE. The effect of reticuloendothelial blockade on the blood clearance and tissue distribution of liposomes. Biochim Biophys Acta 1981;674:354–71. [PubMed: 6165399]
37. Huang SK, Mayhew E, Gilani S, Lasic DD, Martin FJ, Papahadjopoulos D. Pharmacokinetics and therapeutics of sterically stabilized liposomes in mice bearing C-26 colon carcinoma. Cancer Res 1992;52:6774–81. [PubMed: 1458465]
38. Mazurchuk R, Zhou R, Straubinger RM, Chau RI, Grossman Z. Functional magnetic resonance (fMR) imaging of a rat brain tumor model: implications for evaluation of tumor microvasculature and therapeutic response. Magn Reson Imaging 1999;17:537–48. [PubMed: 10231180]
39. Maeda H, Wu J, Sawa T, Matsumura Y, Hori K. Tumor vascular permeability and the EPR effect in macromolecular therapeutics: a review. J Control Release 2000;65:271–84. [PubMed: 10699287]
40. Huang SK, Lee KD, Hong K, Friend DS, Papahadjopoulos D. Microscopic localization of sterically stabilized liposomes in colon carcinoma-bearing mice. Cancer Res 1992;52:5135–43. [PubMed: 1394121]
41. Gabizon A, Price DC, Huberty J, Bresalier RS, Papahadjopoulos D. Effect of liposome composition and other factors on the targeting of liposomes to experimental tumors: biodistribution and imaging studies. Cancer Res 1990;50:6371–8. [PubMed: 1698120]

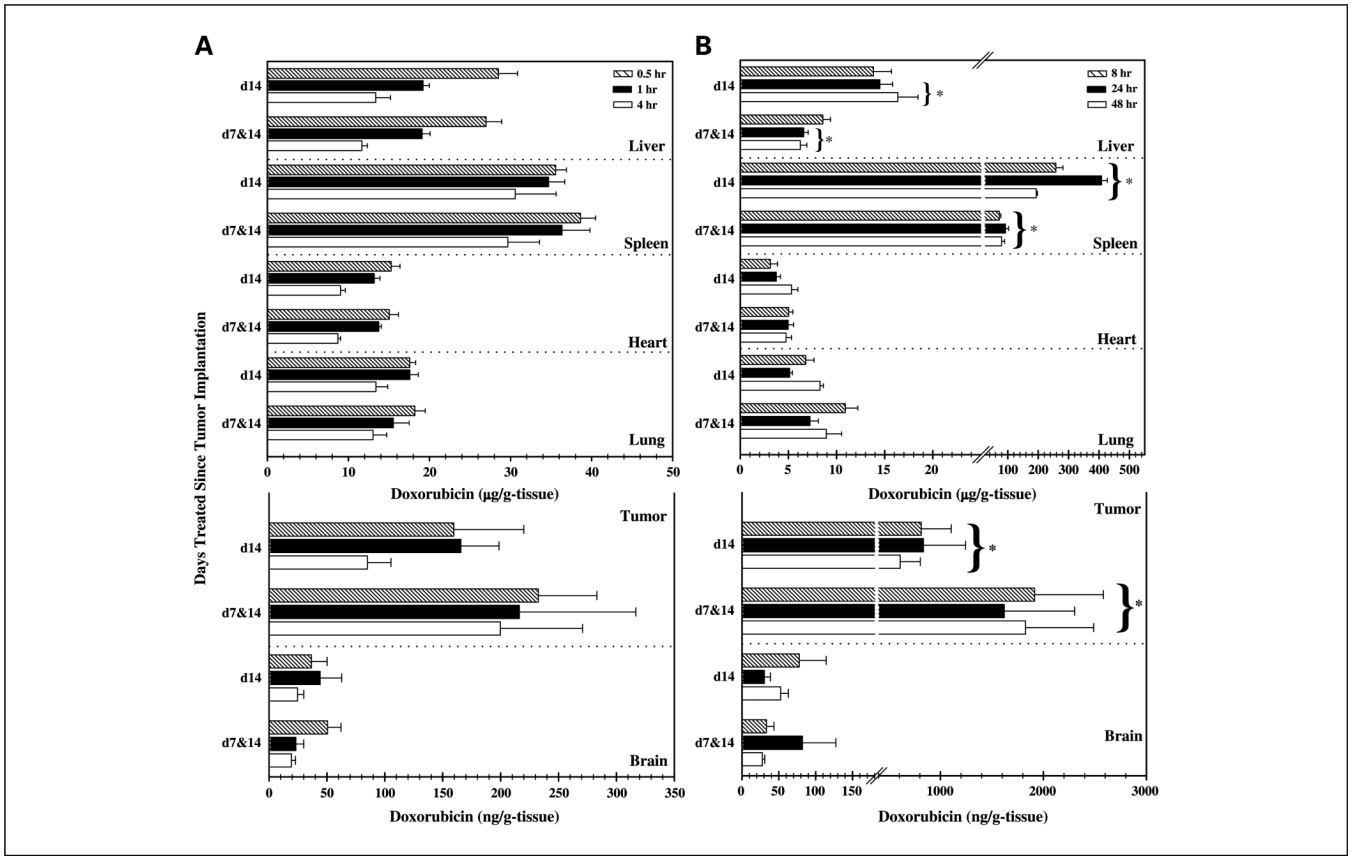

Fig. 1.

Biodistribution of doxorubicin after single and repetitive treatments. *A*, tissue and tumor biodistribution of doxorubicin after single (day 14) and repetitive (days 7 and 14) i.v. doses of 5.67 mg/kg free doxorubicin. *B*, tissue and tumor biodistribution of doxorubicin after day 14 (*d14*) and days 7 and 14 (*d7*&*d14*) administration of 5.67 mg/kg SSL-DXR. Columns, mean (n = 4-8 animals); bars, SE. For animals treated on days 7 and 14 with SSL-DXR, a significant decrease in liver deposition was observed at 24 and 48 hours and in spleen deposition at 8, 24, and 48 hours. Naive pooled data analysis showed that repetitive administration of SSL-DXR significantly increased the cumulative brain tumor deposition compared with a single treatment. Temporal and treatment-mediated differences in drug deposition were tested in SAS using a stepwise two-way (time and treatment) ANOVA followed by a post hoc Bonferroni t test. *, $P < 0.05$.

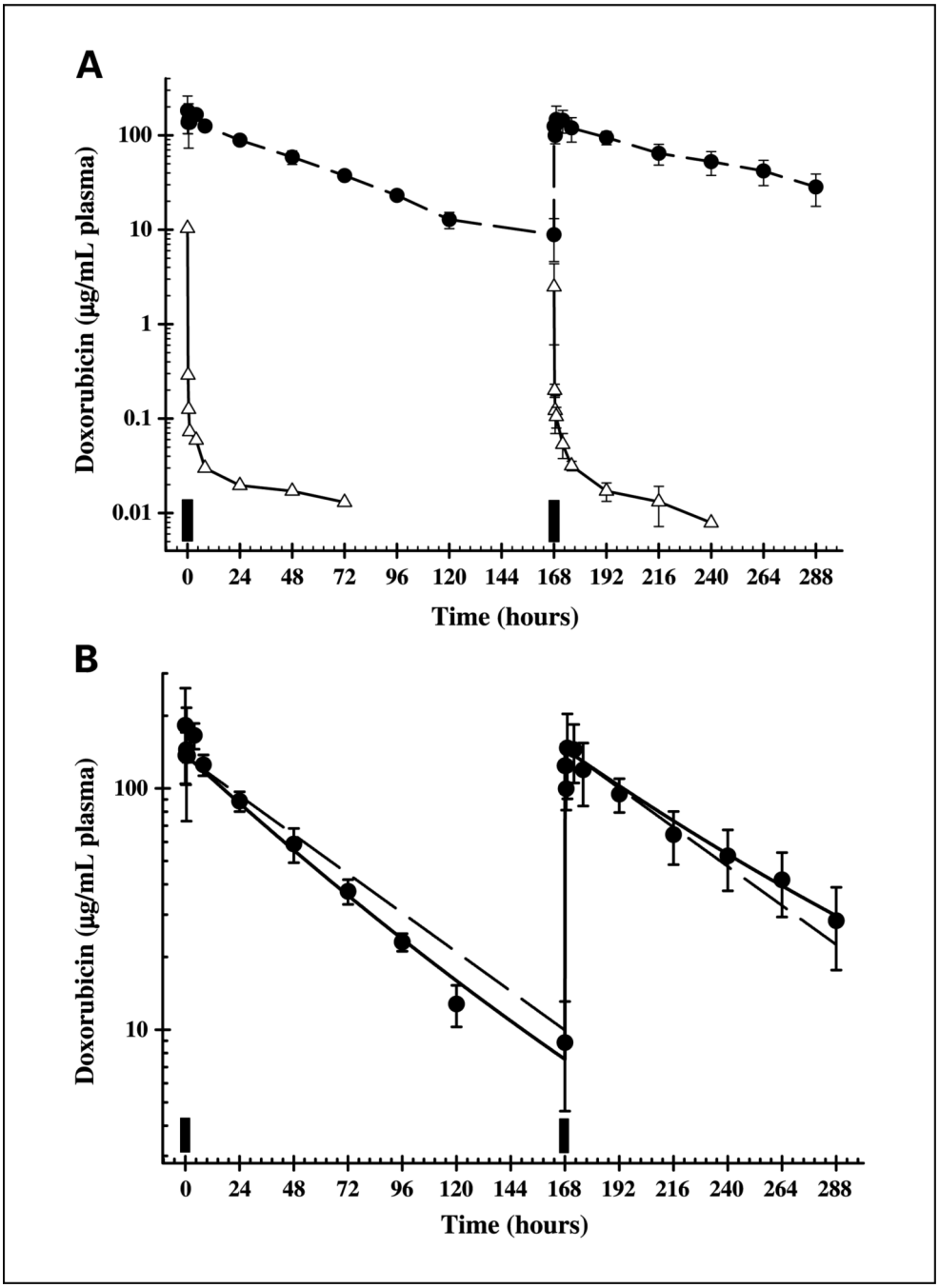

Fig. 2.

Observed and model-predicted plasma pharmacokinetics of doxorubicin. *A*, concentration-time profiles of doxorubicin in plasma after administration of 5.67 mg/kg free doxorubicin (△ and *solid lines*) or SSL-DXR (• and *dashed lines*). Filled bars, time of administration. Points, mean of three to five individual animals at each time point; bars, SD. Lines are drawn point-to-point. *B*, doxorubicin plasma concentrations were analyzed using pharmacokinetic models developed to fit simultaneously the data for both single and two weekly doses of SSL-DXR. •, SSL-DXR-treated animals as shown in (*A*). Solid line, fit of the model described by Eq. A to the data, in which the initial rate of elimination (*k*) is hypothesized to decrease incrementally

with time (according to the variable α) as a response to the first dose. Dashed line, fit of the model under conditions of stationary kinetics (α = 0), in which the elimination rate is held constant for both doses of SSL-DXR.

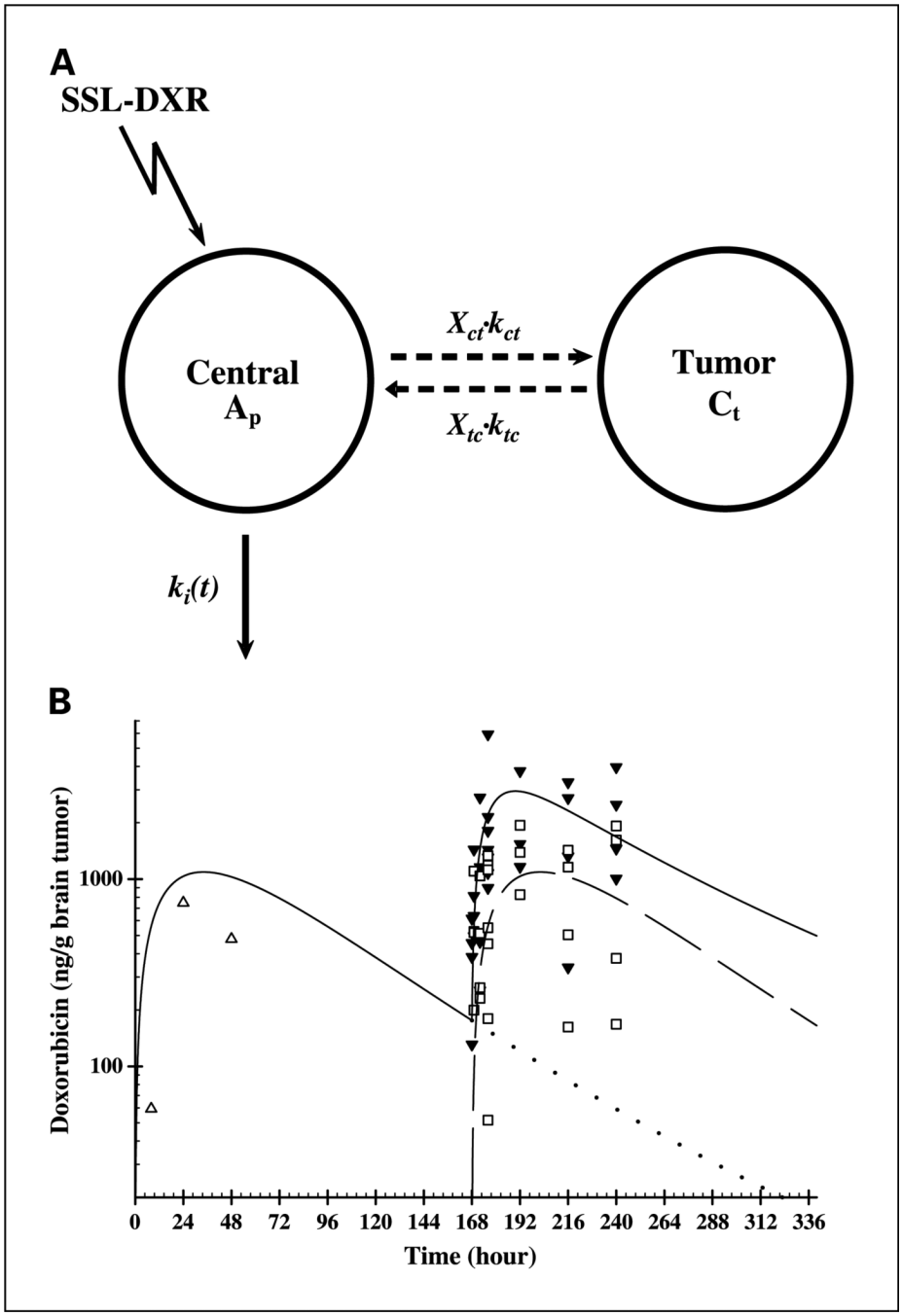

Fig. 3.

Observed tumor deposition of SSL-DXR and deposition predicted by a pharmacokinetic model. *A*, a pharmacokinetic model designed to fit simultaneously the brain tumor concentrations observed resulting from single and repetitive treatment with SSL-DXR (*SSL-DXR*). The concentration of drug in tumor (Ct) was described using a one-compartment model (Eq. B) in series with fixed plasma concentrations (Eq. A), where k_{ct} and k_{tc} are the first-order rate constants for uptake and elimination between the plasma and the tumor, respectively. A scaling factor that accommodates stepwise changes in variables from different cohorts permitted simultaneous fitting of all treatment groups and was used to estimate the magnitude of change in the uptake rate (X_{ct}) or elimination rate (X_{tc}) mediated by repetitive administration

of SSL-DXR. *B*, observed and model-predicted brain tumor concentrations following single or repeat weekly administration of SSL-DXR. Open symbols, observed tumor concentrations following a single treatment given on day 7 (△) or day 14 (□); filled symbols, tumor concentrations observed following the second of two SSL-DXR administration [i.e., days 7 and 14 (▼)]. Solid line, model prediction after single (day 7) and repetitive (days 7 and 14) treatment with SSL-DXR; dashed line, model fit of data from animals that received a single day 14 treatment; dotted line, model prediction for the residual SSL-DXR in brain tumors 168 to 336 hours after the administration of SSL-DXR on day 7.

Table 1

Observed and model-predicted effect of single or repeat SSL-DXR treatment on brain tumor drug exposure in rats

Treatment	SSL-DXR in tumor mean$_{168\text{-}240\ h}$ ± SE (ng doxorubicin/g tumor)	Tumor AUC$_{168\text{-}240\ h}$ for SSL-DXR (μg doxorubicin h/g tumor)	
	Naive average data	Observed	Model predicted
Single (day 7 or 14)*	769 ± 145	57.5	63.7
Repetitive (days 7 and 14)†	1,760 ± 260‡	129	159
% Change	228	225	250

*Rats were treated with 5.67 mg/kg SSL-DXR either on day 7 (n = 1 at each time point) or day 14 (n = 4-8 at each time point).

†Rats were treated on days 7 and 14 with 5.67 mg/kg SSL-DXR (n = 4-8 at each time point).

‡P values ≤0.05 were considered significant in the comparison of single (day 7 or 14) versus repetitive (days 7 and 14) treatment.

Table 2

Plasma pharmacokinetics of doxorubicin after administration of SSL-DXR (5.67 mg/kg) to rats

Noncompartmental analysis			
Variables	**Single dose mean (CV%)**	**Second dose mean (CV%)**	**Percentage difference**
C_{max} (μg/mL)	205 (31.5)	170 (25.1)	–17.1
k (h^{-1})	0.0191 (8.10)	0.0126* (12.8)	–33.8
$t_{1/2}$ (h)	36.4 (8.17)	55.5* (11.9)	52.3
AUC (mg · h/mL)	7.54 (6.28)	9.74† (19.4)	29.1
V (mL/kg)	40.0 (13.5)	44.0 (22.6)	10.0
CL (mL/h/kg)	0.733 (7.87)	0.560 (27.1)	–23.6

Model-predicted pharmacokinetic variables			
Variables	**Naive pooled data (CV%)**	**Naive averaged data (CV%)**	**Standard two-stage (CV%)**
k_i (h^{-1})	0.0217 (4.41)	0.0197 (3.3)	0.0180 (22.4)
V (mL/kg)	42.5 (4.02)	40.7 (3.3)	43.0 (21.8)
α (h^{-2})	3.74×10^{-5} (14.4)	2.89×10^{-5} (14.5)	1.88×10^{-5} (64.5)‡

Abbreviations: C_{max}, maximum plasma concentration; k, elimination rate; $t_{1/2}$, half-life; AUC, area under the plasma concentration-time curve; V, apparent volume of distribution; CL, total systemic clearance; k_i, initial elimination rate of doxorubicin; α, an empirical scaling factor that decreases k_i linearly with time.

*P values ≤ 0.05 were considered significant.

†The AUC was corrected for residual doxorubicin from first treatment; CV% for naive pooled data and naive averaged data are of the estimated value, whereas the CV% for the standard two-stage is of the population mean.

‡n = 5 animals.

Table 3

Model-predicted rates of brain tumor influx and efflux of doxorubicin after single or multiple doses of SSL-DXR (5.67 mg/kg) in rats

Variable estimates	Single treatment (day 7 or 14)	Two weekly treatments (days 7 and 14)
k_{ct}, h^{-1} (CV%)	6.93×10^{-4} (26.7)	2.83×10^{-3} (24.4)*
k_{tc}, h^{-1} (CV%)	4.67×10^{-2} (39.15)	0.103 (30.0)*
X_{ct} (CV%)	NA	4.1-fold (36.0)
X_{tc} (CV%)	NA	2.2-fold (46.2)

Abbreviations: k_{ct}, tumor influx rate; k_{tc}, tumor efflux rate; X_{ct}, influx multiplicative coefficient; X_{tc}, efflux multiplicative coefficient; NA, not applicable.

*The influx and efflux rates of doxorubicin in brain tumors after repetitive administration of SSL-DXR were estimated as secondary variables in ADAPTas the product of the multiplicative coefficient and the respective rate [e.g., k_{ct} (repetitive) = $X_{ct} \times k_{ct}$ (single)].